



**CHALMERS**  
UNIVERSITY OF TECHNOLOGY

## **Single Particle Plasmonics for Materials Science and Single Particle Catalysis**

Downloaded from: <https://research.chalmers.se>, 2022-01-01 18:33 UTC

Citation for the original published paper (version of record):

Alekseeva, S., Nedrygailov, I., Langhammer, C. (2019)

Single Particle Plasmonics for Materials Science and Single Particle Catalysis

ACS Photonics, 6(6): 1319-1330

<http://dx.doi.org/10.1021/acsphotonics.9b00339>

N.B. When citing this work, cite the original published paper.

# Single Particle Plasmonics for Materials Science and Single Particle Catalysis

*Svetlana Alekseeva, Ievgen I. Nedrygailov and Christoph Langhammer\**

*Department of Physics, Chalmers University of Technology, S-412 96 Göteborg, Sweden*

\*E-mail: clangham@chalmers.se

## ABSTRACT

Single particle nanoplasmonic sensing and spectroscopy is a powerful and at the same time relatively easy-to-implement research method that allows monitoring of changes in the structure and properties of metal nanoparticles in real time and with only few restrictions in terms of surrounding medium, temperature and pressure. Consequently, it has been successfully used in materials science applications to, for instance, reveal the impact of size and shape of single metal nanoparticles on the thermodynamics of metal hydride formation and decomposition. In this Perspective, we review and discuss the research efforts that have spurred key advances in the development of single particle nanoplasmonic sensing and spectroscopy as a research tool in materials science. On this background we then assess the prospects and challenges towards its application in single particle catalysis, with the aim to enable *operando* studies of the relationship between metal nanoparticle structure or oxidation state, and catalytic performance.

Keywords: Single particle plasmonics, single particle catalysis, dark field scattering spectroscopy, materials science, sensing, hydrogen

Heterogeneous catalysis is an integral part of modern society for which it provides highly efficient synthesis routes for chemicals and fuels, as well as solutions for environmental cleanup<sup>1-2</sup>. At the core of modern catalyst systems are complex, multi-component materials that often consist of metal nanoparticles deposited on a support with large specific surface area. They are typically operated at harsh chemical conditions that may range from high temperatures and pressures to chemically oxidizing, corrosive or reducing environments. Hence, the non-invasive, real time, high-resolution (both in space and time) characterization of catalyst nanomaterials at relevant operating conditions – *in operando* – is to this day still one of the holy grails in catalysis research since it constitutes a massive experimental challenge. Consequently, significant efforts have been invested in the development of experimental methods that enable *operando* studies of catalyst materials, and great progress has been made in this respect<sup>3-8</sup>. The made findings all highlight the importance of *operando* studies since they paint a clear picture of a catalyst being a very dynamic system, which continuously evolves its properties both at (very) short and long time scales, in intimate interplay with its surrounding environment and the applied reaction conditions. For example, during reaction, catalyst nanoparticles may dynamically transform their structure<sup>9-11</sup>, sinter and coalesce<sup>12</sup>, melt<sup>13</sup>, corrode<sup>14</sup>, or oxidize at the surface or all the way in the bulk<sup>15-16</sup> (**Figure 1a**).

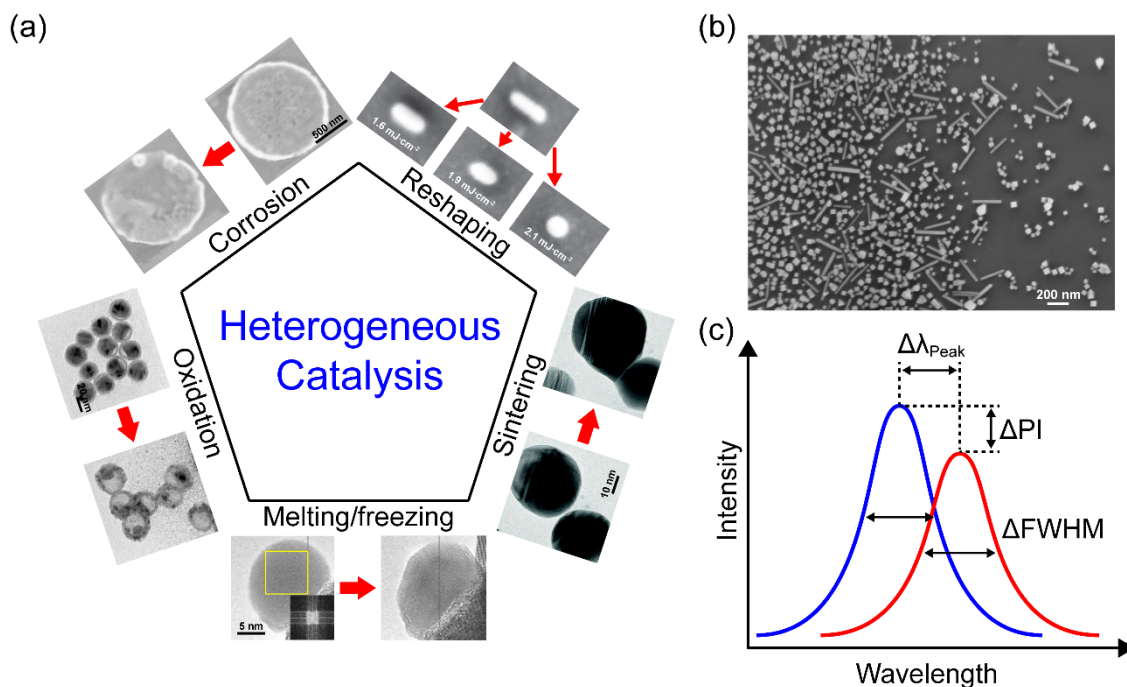


**Figure 1.** (a) Characteristic processes occurring with metal nanoparticles under catalytic reaction conditions. (b) SEM image of colloidal Pd nanoparticles synthesized by adapting procedures described in Ref.<sup>17</sup> and dispersed on a Si substrate by drop-casting. We note the wide variety of obtained sizes and shapes. (c) Basic principle of nanoplasmonic sensing: Transformations in the size, shape or composition of a nanoparticle under the influence of external factors lead to changes in the optical scattering spectrum of the nanoparticle, such as spectral shift of the peak position ( $\Delta\lambda_{Peak}$ ), variation in peak intensity ( $\Delta PI$ ) and changes in full-width-at-half-maximum ( $\Delta FWHM$ ). Reproduced with permission from<sup>10, 12-15</sup>.

A second main challenge in catalysts science and investigations of the active nanoparticles is ensemble averaging, which significantly blurs our vision when, for example, establishing structure-activity/selectivity correlations. The reason is that heterogeneity in terms of size, shape, microstructure and chemical composition (e.g. in the case of alloys or other types

of heterostructures<sup>18-19</sup>) is a general feature among nanoparticles both at the nanometer and at the atomic level (**Figure 1b**), and that activity is non-uniform even across a single particle<sup>20</sup> due to the existence of surface sites with different activity. This heterogeneity hampers the generation of deeper understanding for how these structural parameters affect catalytic activity since they, together with electronic and spill-over interactions with the support, directly control the catalytic performance. In response, over the last decade the field of “single particle catalysis” has emerged in the quest to develop experimental methods that overcome the ensemble averaging problem and even reach single molecule resolution<sup>21-24</sup>. Also in this area significant progress has been made and fascinating insights have been reached using approaches based on super-resolution fluorescence microscopy<sup>20</sup>, tip-enhanced Raman spectroscopy<sup>25</sup>, *in situ* transmission electron microscopy<sup>11</sup> and *in situ* X-ray absorption spectromicroscopy<sup>26</sup>.

In the context of single particle catalysis, conceptually, nanoplasmonic sensing based on dark-field scattering spectroscopy<sup>27</sup> immediately appears as a potentially interesting further contender due to the fact that, when projected onto catalysis research, it provides the possibility to address individual nanoparticles in the 10 – 100 nm size regime. This range is accessible both to the enhanced precision of top-down nanofabrication that enables the preparation of controlled and precisely tunable model systems<sup>28-29</sup>, and to shape-selected synthesis of colloidal nanocrystals<sup>30-31</sup>. Importantly, the single nanoparticle resolution offered by single particle plasmonic sensing comes without principle restrictions on both temperature and the surrounding medium, that is, both liquid and gas phase environments are accessible at ambient pressure or above. Moreover, multiple individual nanoparticles can be addressed simultaneously using concepts like hyperspectral imaging<sup>32-35</sup>. Finally, and as a key point, essentially all the dynamic catalyst nanoparticle transformations highlighted above are perturbing the surface or the bulk of

a catalyst nanoparticle significantly enough by either inducing structural changes to size and shape, or by imposing chemical changes, such as oxidation state, that a significant and measurable change of the localized surface plasmon resonance (LSPR) can be expected.

Relaxing temporarily the single particle boundary condition for the sake of this introductory discussion, it is interesting to provide a brief overview of established applications of LSPR based sensing and spectroscopy. Such a survey shows that this highly sensitive, non-invasive concept has found widespread application in biological sensing, gas detection and materials science applications<sup>36-39</sup>. In the materials science area, relevant application examples include studies of polymer swelling<sup>40</sup>, hydride formation/decomposition<sup>41-43</sup>, phase- and glass transitions<sup>44-48</sup>, corrosion<sup>49</sup>, sintering<sup>50-51</sup>, recrystallization<sup>52</sup>, molecular diffusion in materials<sup>53</sup>, and the melting and growth of nanoparticles<sup>10, 54-55</sup>. As the key conclusion from this summary we highlight the apparent flexibility of nanoplasmonic sensing and spectroscopy in terms of materials that can be studied, the nature of the environment the studies were conducted in, and the relative simplicity of the necessary instrumentation.

In the remainder of this Perspective we will now summarize and discuss the state of the art of applying single particle plasmonic nanospectroscopy and sensing<sup>27, 56</sup> in materials science on the example of metal nanoparticle – hydrogen interactions. Based on these examples that illustrate the potential, we will then outline the way forward towards single particle plasmonics for single particle catalysis, as part of the quest towards a new experimental paradigm where catalyst materials are studied *in operando* at the single nanoparticle level.

## Localized Surface Plasmon Resonance Single Particle Sensing and Spectroscopy

The basic principle of nanoplasmonic sensing is illustrated in **Figure 1c**. When light from the UV-vis-NIR spectral range interacts with a metal nanoparticle with dimensions comparable to or smaller than the wavelength of light, resonant collective oscillations of electrons can be induced<sup>57</sup>. As a result, distinct peaks at the plasmon resonance frequency are observed in absorption and scattering spectra of metal nanoparticles. Since the resonance frequency depends on particle size, shape and composition, as well as the particle surrounding, the typical descriptors used to characterize plasmonic peaks in optical spectra (that is, peak position, peak intensity and peak spectral line-width) exhibit measurable changes under the influence of external factors<sup>58-60</sup>. These changes can be monitored at the single particle level via dark-field scattering spectroscopy, which provides a straightforward method for highly sensitive detection of transformations occurring with, on, or in the close vicinity of metal nanoparticles. The principle of operation of dark-field microscopy is schematically shown in **Figure 2**. The microscope's dark-field condenser is designed in such a way that only light scattered by the sample can reach the used detector. At the same time, the light that is used to illuminate the sample is not collected by the objective lens and, therefore, is not part of the image, see **Figure 2a**. Such a scheme, despite its simplicity, allows obtaining images with significant contrast that makes it possible to observe and study individual metal nanoparticles in real time across a wide range of conditions. A typical image obtained with dark-field microscopy is shown in **Figure 2b**. Here one can see an array of plasmonic Cu nanoparticles with a diameter in the range of 80-120 nm, nanofabricated on an oxidized silicon surface.

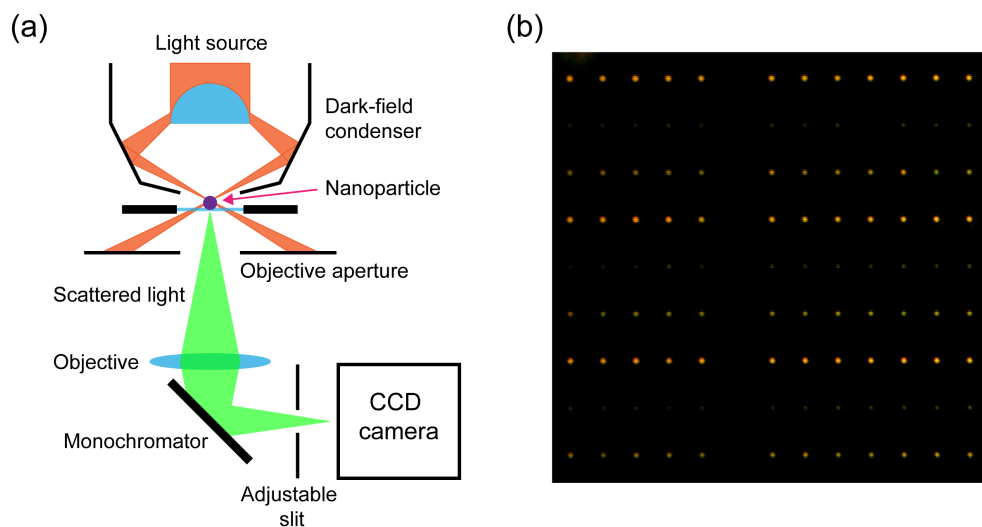


**Figure 2.** (a) Schematic depiction of the dark-field scattering microscopy principle. (b) True-color dark-field microscopy image of electron beam lithography fabricated metallic Cu nanoparticles with diameters in the range of 80-120 nm.

### Metal Nanoparticle – Hydrogen Interactions

An early and by now mature example of the successful use of the single particle plasmonic sensing and spectroscopy approach in materials science is the case of hydrogen sorption and hydride formation in Pd nanoparticles<sup>39, 41</sup>, a process which today is widely considered for the development of next generation optical hydrogen sensors<sup>61-64</sup>. The seminal paper by Langhammer and co-workers<sup>41</sup> describes a nanoplasmonic hydrogen sensor composed of an array of Pd nanodisks with a diameter of several hundred nanometers, supported on a transparent substrate (**Figure 3a**). Mechanistically, the detection of hydrogen uptake relies on the fact that the LSPR frequency of a hydride-forming metal nanoparticle is proportional to the amount of hydrogen absorbed throughout the  $\alpha$ -phase region at low-hydrogen partial pressure where hydrogen is diluted at low concentration in a solid solution, which is characterized by very weak hydrogen-hydrogen interaction; the  $\alpha + \beta$ -phase-coexistence region (“plateau”) at the first-order



phase transition to and from the hydride ( $\beta$ -phase); and finally, the pure  $\beta$ -phase region at high-hydrogen partial pressure<sup>42, 65</sup>.

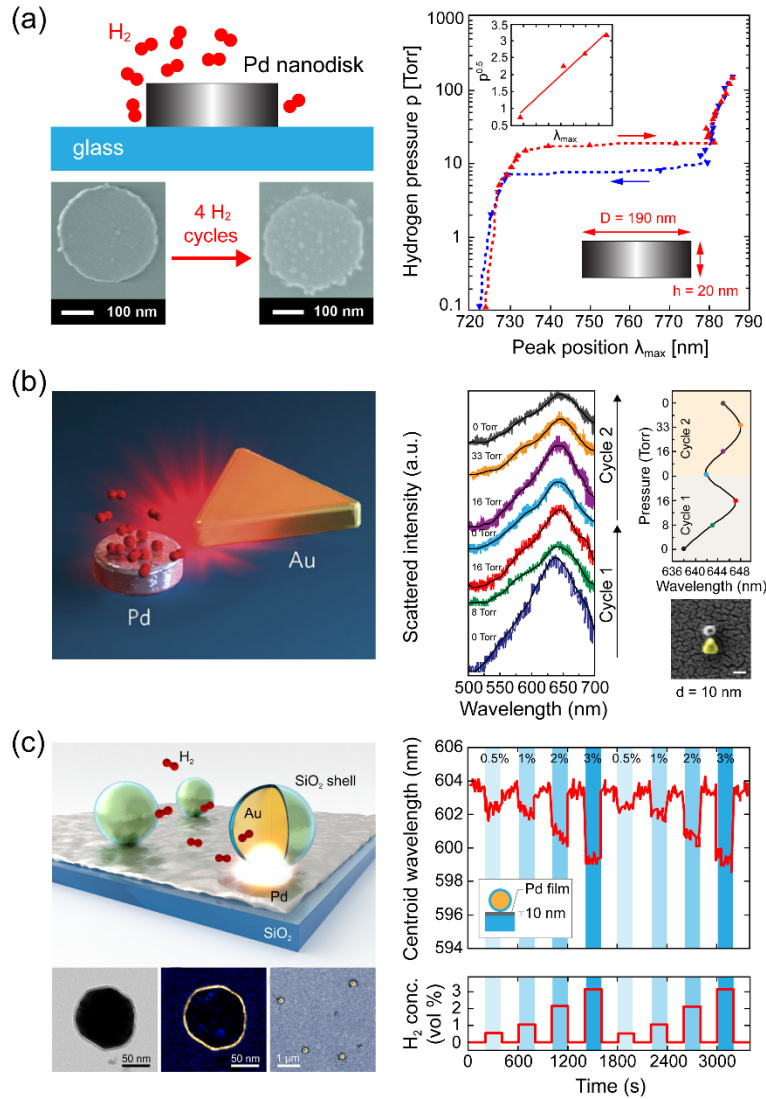


**Figure 3.** (a) Left panel: SEM images of a single Pd nanodisk before interaction with H<sub>2</sub> and after four cycles of H<sub>2</sub> uptake and release at room temperature. The structural changes around the edges of the Pd nanodisk are due to crack formation during H<sub>2</sub>-induced expansion and contraction. Right panel: Optical p - λ<sub>max</sub> isotherms for H<sub>2</sub> uptake and release in an array of Pd

nanodisks. Inset: optical response for the Pd-H system consistent with Sievert's law in the hydrogen solid solution regime, indicating direct proportionality between plasmonic peak position,  $\lambda_{max}$ , and amount of hydrogen absorbed into the Pd nanodisks. (b) Left panel: Schematic of Au plasmonic antenna-enhanced sensing of H<sub>2</sub> absorbed into a single Pd nanoparticle. Right panel: Optical scattering measurements of a system composed of a single Pd nanoparticle located at a distance of 10 nm from the triangle Au antenna. (c) Left panel: The principle of probing interactions of H<sub>2</sub> with the surface of a Pd film using plasmonic smart dust. Right panel: Time-resolved measurements of centroid wavelength position of a single smart dust particle upon interaction of the 10 nm thick Pd film with H<sub>2</sub>. Reproduced with permission from<sup>41</sup>, 66-67

After the introduction of this plasmonics-based scheme for the study and detection of metal-hydrogen interactions, Liu et al.<sup>66</sup> and Shegai et al.<sup>68</sup> demonstrated almost simultaneously the possibility to detect hydrogen sorption and hydride formation in single Pd and Mg nanoparticles. However, due to the intrinsically small scattering cross sections of Pd<sup>69</sup> rendering direct dark-field scattering spectroscopy challenging, they applied an indirect detection scheme previously demonstrated for nanoparticle ensembles<sup>47</sup> using a single Au plasmonic nanoantenna adjacent to the single hydride forming Pd nanoparticle. In this arrangement, the nanoantenna probes and signals the hydride formation process via its near-field and via scattering to the far-field, respectively (**Figure 3b**). Specifically, due to the small distance separating the nanoantenna and the Pd nanoparticle, the optical properties of the entire complex change when Pd sorbs hydrogen, due to the concurrent change in both volume and electronic properties of the Pd<sup>65, 70</sup>. This causes a shift of the LSPR in the single particle scattering spectrum of the coupled

Pd-Au system, which can be detected using dark-field scattering spectroscopy (**Figure 3b** right panel). Similar studies using different variations of the indirect sensing principle have further corroborated the approach as such, and helped to shed light on nanoparticle size and shape effects<sup>71</sup> or on hydrogen sorption in Pd thin films using the concept of so-called plasmonic smart dust<sup>67</sup>. In the latter study, the smart dust consisted of dielectric shell-isolated gold nanoparticles distributed over the surface of the Pd film to locally probe uptake and release of hydrogen (**Figure 3c**). Sizable spectral shifts of the resonance peak were detected upon interaction of the Pd film with hydrogen, again highlighting the unique ability of single particle plasmonic sensing to investigate chemical transformations. We also note that a very similar mechanism is widely used in Core-Shell Nanoparticle-Enhanced Raman Spectroscopy (SHINERS)<sup>72</sup>.

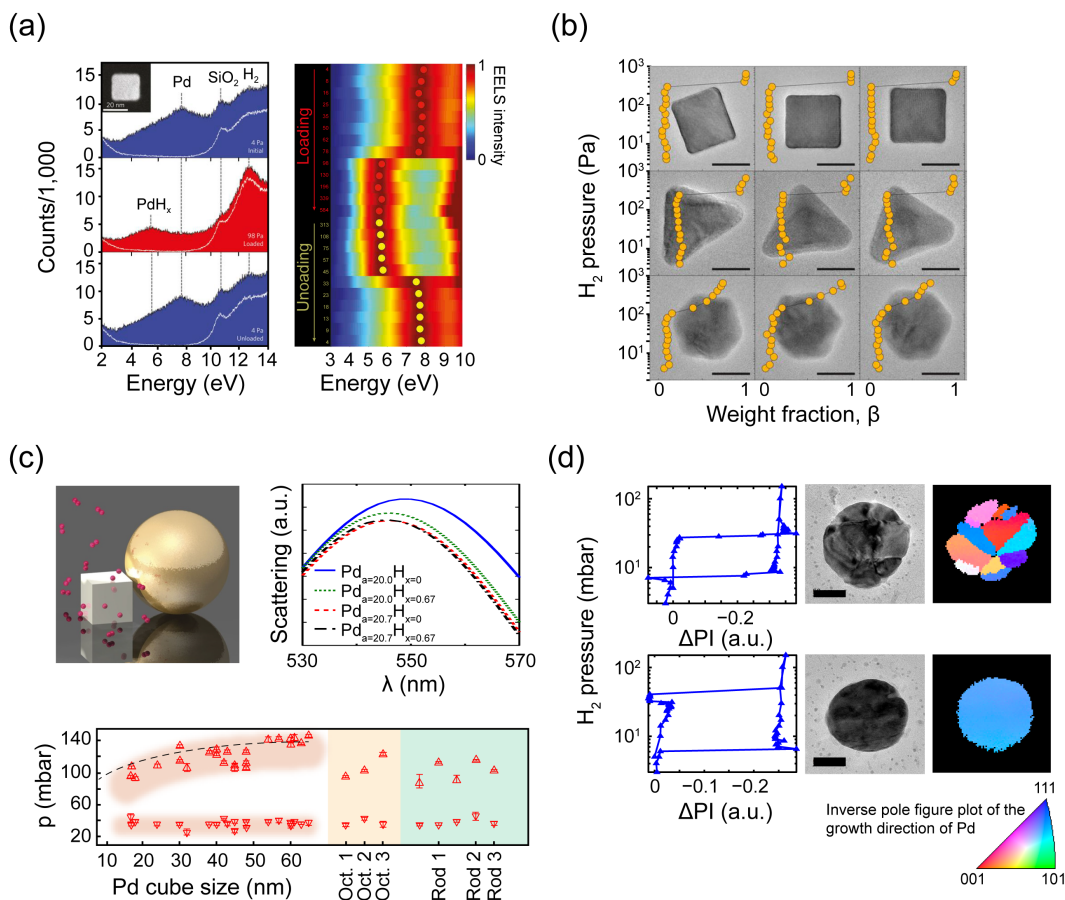


**Figure 4.** (a) EEL spectra recorded on a single Pd nanocube with edge length of 23 nm before and after hydrogen absorption. Scale bar is 20 nm (b) Pseudo pressure-composition isotherms and corresponding high-resolution TEM images after H<sub>2</sub> absorption and desorption for single Pd nanocubes, pyramids, and icosahedra. Scale bars are 20 nm. (c) Top panel: Schematic of a heterodimer composed of a nanoplasmonic Au antenna combined with a Pd nanocube and corresponding FDTD simulations of the light scattering by various Au-Pd heterodimers upon hydrogen sorption in the Pd element. Bottom panel: Equilibrium pressures for hydride formation (upward pointing triangles) and decomposition (downward pointing triangles) for single Pd nanocubes, octahedra and nanorods of various size, measured by the heterodimer method. (d) Optical pressure-composition isotherms for hydrogen sorption in individual, polycrystalline Pd nanoparticles and corresponding TEM and Transmission Kikuchi Diffraction (TKD) images. Scale bar is 50 nm. Reproduced with permission from<sup>73-76</sup>.

Since these initial proof-of-concept measurements using various nanoplasmonic antennas and hydride forming nanoparticle arrangements<sup>66, 68, 71, 77</sup>, the generic methodology has further evolved into a powerful materials science tool that comes in various sophisticated versions. For example, a series of studies by the Dionne group elegantly exploited *in situ* Electron Energy-Loss Spectroscopy (EELS) and Transmission Electron Microscopy (TEM) to study the hydride formation process in various types of size- and shape-selected Pd nanocrystals by exciting plasmonic resonances with the electron beam and tracking the corresponding change in measured energy loss as a function of hydrogen sorption<sup>71, 73-74, 78-81</sup>. A typical result from their seminal study<sup>73</sup> is shown in **Figure 4a** where raw EEL spectra recorded on a 23 nm Pd nanocube are

shown before and after hydrogen absorption. A shift of the bulk resonance peak of about 2 eV caused by hydrogen absorption and desorption is clear evidence of hydrogenation and dehydrogenation taking place in the Pd nanocube. In a follow up study, the spatial distribution of phases present during hydride formation in single nanocrystals with different shapes was reconstructed, using a combination of EELS, dark-field imaging and electron diffraction<sup>74</sup>. Corresponding pseudo pressure-composition isotherms based on the spectral contribution of each phase, extracted from EELS data and plotted versus the weight fraction of the  $\beta$  phase,  $\beta/(\alpha + \beta)$ , are shown in **Figure 4b** for Pd nanocubes, pyramids, and icosahedra.

Another type of example for the use of single particle plasmonics to study the thermodynamics of hydride formation in individual Pd nanoparticles with different shapes and sizes was presented by Syrenova et al.<sup>75, 77</sup>. For this purpose, an electrostatic heterodimer self-assembly method was first developed, to enable the controlled formation of Au nanoantenna – Pd nanocrystal heterodimers (**Figure 4c**). From the dark-field scattering spectra of individual Au-Pd heterodimers it becomes evident that the transition of the Pd nanoparticle from the metallic to the hydride phase is accompanied by a clear shift of the scattering peak to shorter wavelengths. As one of the key results, this study revealed that the characteristic slope found across the plateau in the phase transformation region of pressure-composition isotherms measured for Pd nanoparticle ensembles is the consequence of significantly different phase transformation pressures of the individuals.

As the third example, we present our most recent study, which focused on shedding light on the role of the microstructure in polycrystalline Pd nanoparticles during hydrogen sorption.<sup>76</sup> We employed a direct version of plasmonic sensing, which is based on measuring dark-field scattering spectra of multiple Pd nanoparticles grown on a TEM membrane at the same time

(without adjacent nanoantenna probe), to (i) eliminate experiment-to-experiment artifacts and (ii) enable detailed *ex situ* nanoparticle characterization by high resolution TEM and Transmission Kikuchi Diffraction (TKD). In this way, we were able to demonstrate a direct correlation between the equilibrium pressures for the formation of hydrides in Pd nanoparticles and the length and type of grain boundaries in these nanoparticles (**Figure 4d**).

From the so far presented examples, we can draw a number of intermediate conclusions. For example, it becomes clear that the fascinating differences in the nature of the interaction of Pd nanoparticles and nanocrystals of various shapes sizes and microstructures with hydrogen could only be found due to the single nanoparticle approach. In other words, in similar studies using conventional experimental methods and nanoparticle ensembles, the found effects would have remained hidden. Thus, the single particle studies convincingly demonstrated the capacity of single particle plasmonics as a tool for the detailed and quantitative study of chemical transformations in individual nanoparticles and the value of the obtainable insights.

Secondly, we note that, as highlighted by the last example, single particle plasmonics based on dark-field scattering spectroscopy provides ample opportunities for the parallel readout of multiple individual nanoparticles at exactly identical experimental conditions. This is a very important direction of development, (i) because *serial* measurements on single nanoparticles are prone to artifacts due to, for instance, changing experimental conditions or the investigated process itself altering the nanoparticles over time, and (ii) because, if single particle experiments are to be used to explain trends obtained from ensemble measurements, a large number of individual particles needs to be investigated. Therefore, as part of this Perspective, we now briefly discuss the unique opportunities offered by single particle plasmonics in this respect.

## Multiparticle Plasmonic Nanospectroscopy

In the standard method of measuring a scattering spectrum from a single nanoparticle, it has to be isolated in the field of view of the dark-field microscope, for example by the slit of the spectrometer<sup>27, 56, 82-83</sup>. Thus a first straightforward way to address multiple single nanoparticles simultaneously is to align them along the slit<sup>84-85</sup> of an imaging spectrometer, which can be realized efficiently by, for example, e-beam lithography fabrication<sup>33, 85</sup> allowing for up to 15-20 nanoparticles to be measured at the same time with temporal resolution on the order of 1 to 10 s, depending on the scattering intensity of the nanoparticle that allows for reasonable signal-to-noise ratio. However, these measurements are always limited to the number of particles that can fit vertically in the slit area, as dictated by the diffraction limit. Alternatively, there exist methods for fast parallel spectroscopy that are performed in the wide field of view (not limited by spectrometer slit), which significantly increases the number of particles that can be measured simultaneously. For example, one can detect scattered light over a large field of view using a color camera, and assign pixels to the scattering spots of the particles, and then the approximation with an algorithm of the RGB pixel values results in the scattering peak wavelength<sup>86-87</sup>. The acquisition speed of the images was shown to be below 600 ms per image<sup>86</sup> and can be improved with more advanced cameras. There are also different versions of hyperspectral imaging that allow for measurements of more than 50<sup>32</sup>, 100s<sup>34, 88</sup> and up to 1000<sup>89</sup> nanoparticles simultaneously. However, in these cases the spectra have to be scanned by wavelength and integration times range from  $\sim 0.3$  s to 1 s<sup>32, 34, 88-89</sup> per wavelength (usually with spectral resolution of 1-2 nm). This makes the acquisition time of the already limited spectral range significantly long. Studies of dynamic systems with fast kinetics (such as catalysts usually are) require very high temporal resolution. Currently, this can be achieved by using

monochromatic light illumination (few nm bandwidth) with temporal resolution from 100 ms<sup>90</sup> down to the few ms<sup>91</sup> range, and it is limited only by the signal-to-noise ratio and sampling rates of the photon counting electronics. As one main conclusion we thus identify the need for the reduction of acquisition time for each set of simultaneously measured multiple nanoparticles as an important future challenge for this approach, to enable monitoring of (very) fast processes in the milliseconds down to femtoseconds range, which are relevant in heterogeneous catalysis<sup>92</sup>. A very nice development in this direction has been demonstrated recently, on the example of a method called snapshot hyperspectral imaging. It combines separate and parallel scanning of both spectral and spatial dark-field images from multiple single nanoparticles (up to 100 particles for an ordered array)<sup>35</sup>, and enables an acquisition time of 1 ms with a spectral resolution of 0.21 nm/pixel.



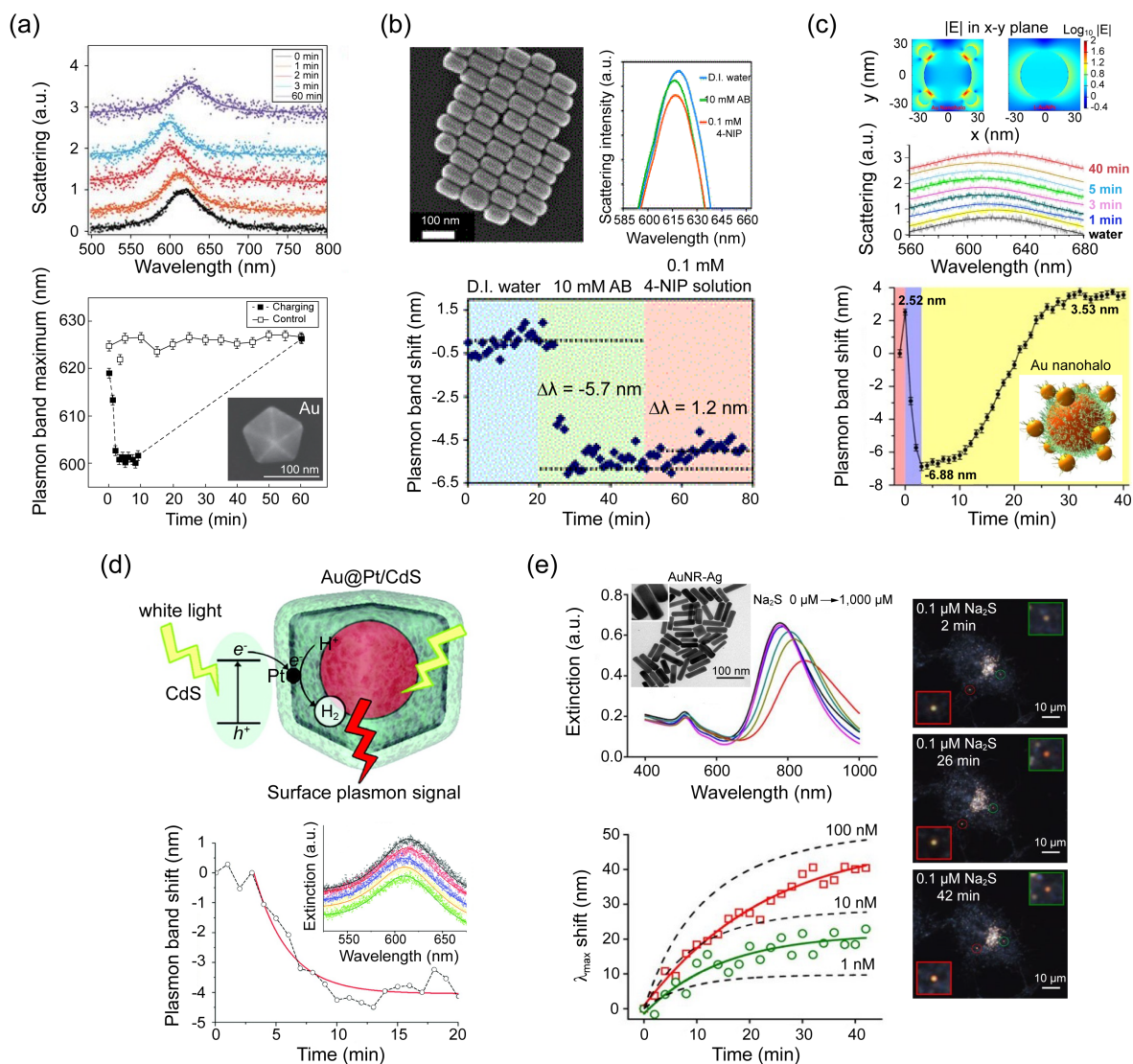


**Figure 5.** (a) Scattering spectra of single Au nanoparticles (top panel) and the corresponding spectral shift as functions of reaction time during the catalytic oxidation of ascorbic acid (bottom panel). The peak shift signal is caused by electron injection into the Au during reaction. Inset: SEM image of the Au decahedron used as the catalyst. (b) Scattering spectra and the surface plasmon band shift of an elongated tetrahedral Au nanoparticle in D.I. water, ammonia borane (AB), and during the reaction of 4-nitrophenol (4-NIP) reduction. The peak shift is caused by charge transfer between reactants and nanoparticles. (c) Top panel: FDTD simulation of the

*local electric field enhancement of a single Au nanohalo (left) and an Au nanosphere (right). Bottom panel: LSPR peak shifts observed along the catalytic reaction between glucose and O<sub>2</sub> on the Au nanohalo. (d) Top panel: Schematic of a single particle measurement of hydrogen evolution on a single Au@Pt/CdS hollow cube. Bottom panel: Plasmon band shift of a single Au@Pt/CdS hollow cube along the photocatalytic decomposition of lactic acid. Inset: Extinction spectrum evolution of a single Au@Pt/CdS cube along the reaction coordinate. The measured peak shift is the consequence of change in the refractive index of the medium surrounding the Au@Pt/CdS particle as a result of the decomposition of lactic acid. (e) Top panel: Extinction spectra of ~50 pM solution with AuNR-Ag core-shell nanoparticles after adding Na<sub>2</sub>S. Bottom panel: Time-dependent shifts of the LSPR peak position ( $\lambda_{max}$ ) of two nanoparticles after adding Na<sub>2</sub>S to the live cell culture medium. The measured peak shift is the consequence of variations in the local refractive index, caused by changes in the molar fraction of Ag<sub>2</sub>S formed in the silver shell. Reproduced with permission from Ref.<sup>93-97</sup>.*

### **Single Particle Catalysis in the Liquid Phase**

Having discussed the evolution of single particle plasmonics in materials science with focus on metal-hydrogen interactions, as well as the current state of the art with respect to multiparticle analysis and data acquisition frequency, in the second part of this Perspective we now focus on its potential in single particle catalysis. To this end, the idea of using nanoplasmonic sensing to study catalytic reactions on individual nanoparticles was implemented for the first time about ten years ago. In the seminal work by Mulvaney and co-workers<sup>93</sup> surface plasmon spectroscopy was used to monitor the oxidation of ascorbic acid catalyzed on the surface of single Au

nanoparticles. **Figure 5a** shows typical scattering spectra for a single Au nanoparticle before and some time after the start of the reaction. A significant blue shift of the plasmonic peak of approximately 20 nm was observed, as a result of electron injection by ascorbate ions during the catalytic reaction. Thus, thanks to its sensitivity to the electron density, the approach enabled the real time monitoring of a catalytic process on a single nanoparticle with the ability to detect reaction rates of just 65 molecules per second.<sup>93</sup> Single particle plasmonic measurements using dark-field microscopy were also used by He and co-workers to investigate the catalytic oxidation of CTAB-stabilized Au nanorods by H<sub>2</sub>O<sub>2</sub> in an acidic environment in the presence of bromide.<sup>98</sup> Another example for the successful application of nanoplasmonic sensing to study catalytic reactions on individual Au nanoparticles was demonstrated by Yi and co-workers.<sup>97</sup> Selected results of this work can be seen in **Figure 5b**. Here, elongated tetrahedral (THH) Au nanoparticles, synthesized by a seed-mediated growth method, show a distinct shift of the surface plasmon peak due to charge transfer during the catalytic reduction of 4-nitrophenol. Furthermore, using the indirect sensing approach based on an inert plasmonic observer, the redox reaction between glucose and oxygen<sup>94</sup>, catalyzed by very small Au spheres could be monitored via larger Au spheres (**Figure 5c**), and the decomposition of lactic acid<sup>95</sup> was measured indirectly on platinized cadmium sulfide through Au patches that served as a scattering probes (**Figure 5d**). Another interesting example is the mapping of sulfide formation inside living cells, which was enabled by single Au nanorod-Ag (AuNR-Ag) core-shell particles<sup>96</sup>. In this arrangement, the Ag acts as an agent reacting with sulfide and the Au nanorod reports the resulting shifts via the scattering signal (**Figure 5e**). In summary, the single particle plasmonic measurements of catalytic reactions described above were able to provide valuable information about reaction rates<sup>93, 95-96</sup>, details of reaction kinetics<sup>98</sup>, the effect of surface facets on catalytic

activity<sup>97</sup>, and changes in surface coverage and charge state of the catalyst<sup>94</sup>, which helped in elucidating the details of the reaction mechanisms and of the catalyst activity at the single nanoparticle level.

While discussing the use of nanoplasmonic sensing for studies of heterogeneous catalysis at the level of individual nanoparticles in liquid environment, we also want to mention a number of works aimed at coupling single particle plasmonics with electrocatalysis. To study the electrocatalytic oxidation of H<sub>2</sub>O<sub>2</sub> on a single Au nanorod, Long and co-workers developed a spectroelectrochemical setup in which a dark-field microscope is combined with a 3-electrode electrochemical cell<sup>99-100</sup>. By tracking the position of the plasmonic peak in the spectrum of scattered light, this setup allowed the authors to observe various processes on the surface of individual Au nanorods in real time. In another study conducted by the same group, a combined spectroelectrochemical setup was used to study changes in the optical properties of individual Au nanorods during electrocatalytic oxidation of glucose in an alkaline medium<sup>101</sup>. Finally, Tschulik and co-workers recently reported on the study of reactivity of individual Ag nanoparticles in aqueous suspensions using an opto- and spectroelectrochemical approach that combines electrochemical dark-field microscopy and hyperspectral imaging<sup>102</sup>. Considering the practical importance of electrocatalysts for use in the energy sector, environment and other applications, further studies in this direction appear very promising.

### **Single Particle Catalysis in the Gas Phase**

Introducing the final section of this Perspective, we note that in all the single particle studies discussed above the catalytic reaction has taken place on nanoparticles immersed in *liquid* solvents and reactants at or close to room temperature. This leaves unaddressed the very

important field of gas phase catalytic reactions, which typically take place at elevated temperatures and at atmospheric pressure or above. Hence, studying such processes sets higher demands both on the used instrumentation and on the applied plasmonic platform to sustain the chemically and thermally harsher conditions. To this end, Larsson et al. demonstrated in a seminal study that the heterostructure schematically depicted in **Figure 6a** enables plasmonic sensing of gas phase catalytic reactions at the ensemble level<sup>103</sup>. The used platform is comprised of an array of Au nanoparticle sensors, encapsulated in a thin dielectric layer for protection and to mimic the oxide support of a typical supported nanocatalyst, onto which small Pt catalyst nanoparticles were grown. This arrangement again uses the plasmonic nanoparticles as inert observers to probe the catalyst via their enhanced near field. Using it, enabled the monitoring of three different common heterogeneous catalytic processes, that is, the oxidation of H<sub>2</sub>, the oxidation of carbon monoxide (CO), and NO<sub>x</sub> reduction and storage. As one of the main results, it was found that changes of the catalyst surface state upon sweeping of the relative reactant concentration could be accurately resolved, including the so-called kinetic phase transition, manifested as a distinct step in the plasmonic signal (**Figure 6a**, bottom panel). Two more recent examples using a similar approach have been presented by Niemantsverdriet et al.<sup>104-105</sup>, where in the second study<sup>105</sup> quadruple mass spectrometry readout was added and directly correlated with the optical response of a Cu nanoparticle ensemble (**Figure 6b**). Despite this demonstrated potential the plasmonic sensing concept – both in its direct and indirect variants – reports on single particle plasmonic experiments in the gas phase are still very scarce, with the only exception of a study of hydrogen spillover effects between a single Au nanorod and a metal oxide support by Mulvaney and coworkers<sup>106</sup>, see **Figure 6c**.

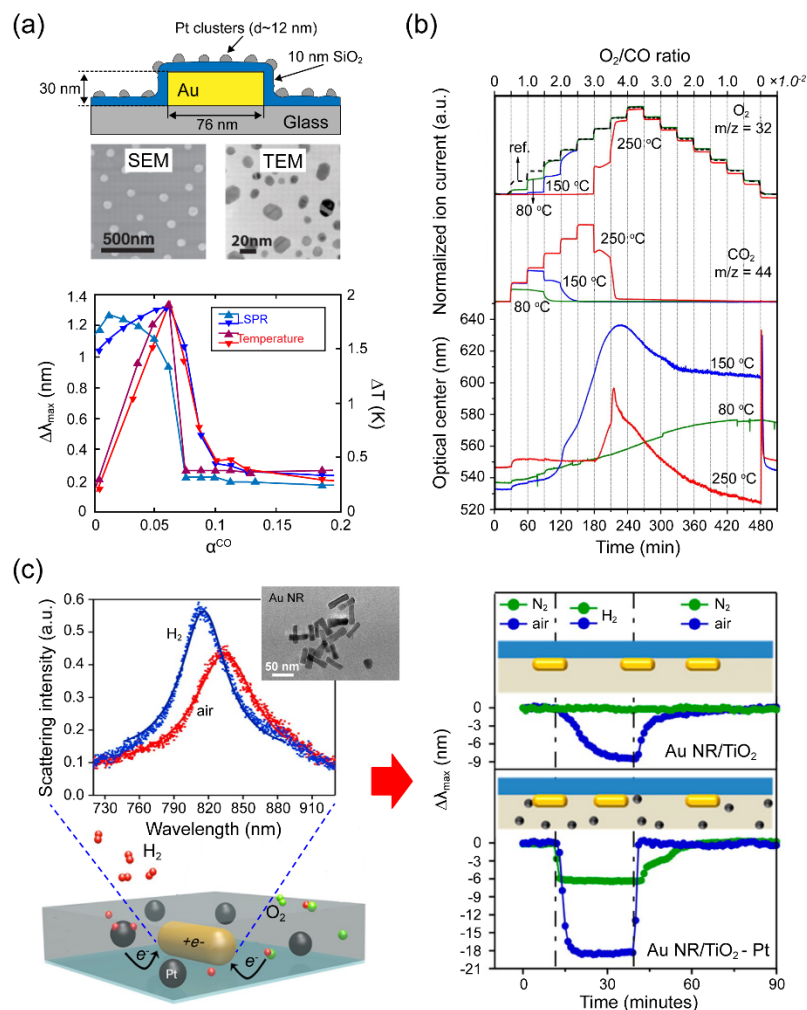


**Figure 6.** (a) Top: Schematics of the nanoarchitecture used to monitor changes in the adsorbate coverage of a Pt catalyst nanoparticle ensemble in operando during the CO oxidation catalytic reaction by adjacent Au plasmonic nanoantenna probes. Also shown are SEM and TEM images of the Au nanoantenna array and the Pt catalyst particles, respectively, used in the sensing structure. Bottom: Plasmon peak shift (blue) and corresponding temperature variation (red) during a sweep of the relative reactant concentration  $\alpha^{CO}$  at  $T = 506$  K. The distinct step in peak shift denotes the kinetic phase transition, at which a sudden change in adsorbate coverage occurs on the catalyst. The origin of the peak shift is not explicitly mentioned. (b) Mass-spectrometric measurements of O<sub>2</sub> and CO<sub>2</sub> during CO oxidation on a Cu nanoparticle catalyst

at different temperatures (top panel) shown together with the optical center position of the Cu nanoparticles, as calculated from *operando* UV-vis measurements (bottom panel). The data reveal a sudden drop in activity as the Cu catalyst gets oxidized and loses its plasmonic response. The measured change in optical center is a consequence of the oxidation of the particles and the corresponding transformation from the metallic to the oxide state with distinctly different optical properties. (c) Left panel: Scattering spectra of a single Au nanorod (NR) embedded in the TiO<sub>2</sub> thin film of the used Au/TiO<sub>2</sub>-Pt sample architecture measured upon exposure to air (red) and H<sub>2</sub> (blue) at room temperature. Right panels: LSPR peak position change measured for a single Au nanorod embedded in Au/TiO<sub>2</sub> (top) and in TiO<sub>2</sub>-Pt (bottom) upon cycling in N<sub>2</sub>-H<sub>2</sub>-N<sub>2</sub> (green lines) and air-H<sub>2</sub>-air (blue lines). The measured peak shift is the consequence of electron injection into the Au NRs during the hydrogen dissociation. Reproduced with permission from Ref.<sup>103, 105-106</sup>

## Future Perspectives

The recent developments in single particle plasmonic sensing and spectroscopy show that this method provides ample opportunities to address individual nanoparticles in the 10 – 100 nm size regime *in operando*, under a wide range of conditions in both the gas and liquid phase. Hence, it can enable the investigation of both nanofabricated and colloidal nanoparticles and structures in an efficient way and in environments of relevance for heterogeneous catalysis. Specifically, as discussed, the plasmonic response of a metal nanoparticle is expected to be sensitive to essentially all possible dynamic catalyst nanoparticle transformations that may occur during reaction, such as shape change, size change (sintering), change of oxidation state, change in the

state of charge, change of chemical composition, change in microstructure, or spill-over effects to the support. This has two key implications: (i) it makes the method very versatile; and (ii) it may render data interpretation challenging if multiple processes occur simultaneously. As a consequence, we foresee that modeling tools such as the Finite-Difference Time-Domain (FDTD) method will have to play a key role in de-convoluting different contributions to a measured single particle plasmonic response. Furthermore, correlative efforts using electron microscopy techniques for initial, intermittent and *post mortem* detailed characterization of the nanostructures will be critical for the derivation of structure-function correlations at the single nanoparticle level<sup>76, 107</sup>.

Another important aspect to consider and further explore is the use of one of the many variants of hyperspectral imaging or similar concepts that have recently become available, since these offer unique opportunities not accessible with established single particle catalysis experimental methods, such as tip-enhanced Raman spectroscopy or *in situ* transmission electron microscopy, that is, the simultaneous monitoring of a multitude of individual nanoparticles. This is, however, critical, because one of the ultimate goals of single nanoparticle studies is to verify structure-activity relationships that will help to improve the catalytic performance of the ensemble typically used in applications. Hence, it is not enough to investigate one particle at the time, but the statistical analysis of thousands of individuals measured simultaneously to minimize measurement-to-measurement artifacts is required to investigate whether the averaged single particle response reproduces the response of an ensemble of similar nanoparticles. Only if this condition is fulfilled, single particle data are truly relevant, and it can, for instance, be ruled out that the fact that a nanoparticle was probed as an individual does not alter its response. The



latter may be the case due to, for example, the (lack of) mass transport effects that may strongly depend on particle proximity in the catalyst and thus impact the measured apparent activity.

Yet another aspect to consider is that many catalysts metals are poor light scatterers<sup>69, 108</sup> and thus, in particular in the sub 50 nm size range relevant for catalysis, it will be very hard to measure directly using dark-field scattering spectroscopy. Hence, it is likely that antenna-enhanced solutions with closely adjacent inert plasmonic observers will have to be used in this regime<sup>66, 75, 109</sup>, or that alternative solutions such as photothermal imaging or interferometric scattering microscopy may become important<sup>110-111</sup>. Along similar lines, we identify the need for the reduction of acquisition time for each set of simultaneously measured multiple nanoparticles as an important future challenge, which becomes increasingly difficult for small scattering cross-sections of the studied nanoparticles. Yet, for catalysis applications it is highly desirable to be able to monitor (very) fast processes in the milliseconds down to femtoseconds range. Hence, we call for further development in this direction both by clever instrument and readout design to, for example, reduce background scattering<sup>112</sup>, and by capitalizing on the development of fast highly sensitive photon detectors. We also predict that the use of 3D sample nanopositioning will become important to reduce noise induced by sample drift, and in this way increase (time)resolution<sup>113</sup>.

The maybe largest yet essentially unexplored potential of single particle plasmonic sensing and spectroscopy lies in gas phase single particle catalysis due to the fact that the method, in principle, appears to be perfectly compatible with the required conditions, such as high temperatures and atmospheric pressure or even above. In this respect, the remote optical readout is a great advantage compared to, for example, tip-probe-based approaches. However, to be able to capitalize on these traits, the design and construction of tailored measurement

chambers is necessary and needs to be combined with dark-field microscopy. Here, some of the obvious challenges to be resolved lie in limiting the temperature to the position of the catalyst in order to not damage the microscope objective, as well as in minimizing or actively eliminating<sup>113</sup> thermally induced drift and sample movement.

Finally, we highlight a unique opportunity offered by the recently presented possibility of combining nanofluidics with single particle plasmonic sensing<sup>33</sup> in the context of single particle catalysis. Specifically, it may offer a solution to overcome the challenge of detection of product molecules formed on a small number of catalyst nanoparticles, which is ultimately necessary to establish structure-activity correlations. In the single nanoparticle limit, the amount of the reaction product produced as a result of a catalytic process falls significantly below the level that can be detected with a sufficient degree of reliability using conventional methods. Hence, as part of a possible solution, we predict that using nanofluidic structures to host catalytic nanoparticles may reduce the internal volume of the “reactor” to the same order as the volume of the catalytic nanoparticle itself, in this way locally, at the individual nanoparticle level, maintaining a concentration of product molecules that is high enough for detection using, for example, fluorescence or scattering methods<sup>114-115</sup>. At the same time, the state of the catalyst nanoparticle can be monitored based on the dynamics of its plasmonic response. Taken altogether, we therefore anticipate that single particle plasmonic sensing will play an increasingly important role in single particle catalysis.

### **Corresponding Author**

\*clangham@chalmers.se.

### **Author Contributions**

The manuscript was written through contributions of all authors. All authors have given approval to the final version of the manuscript.

### **ACKNOWLEDGMENTS**

This work has received funding from the European Research Council (ERC) under the European Union's Horizon 2020 research and innovation programme (678941/SINCAT) and from the Knut and Alice Wallenberg Foundation project 2015.0055.

## REFERENCES

1. Chorkendorff, I.; Niemantsverdriet, J. W., *Concepts of Modern Catalysis and Kinetics*. Wiley-VCH: Weinheim: 2005.
2. Kolasinski, K. W., *Surface Science: Foundations of Catalysis and Nanoscience*. John Wiley & Sons: 2012.
3. Salmeron, M.; Schlögl, R., Ambient pressure photoelectron spectroscopy: A new tool for surface science and nanotechnology. *Surface Science Reports* **2008**, *63*, 169-199.
4. Papp, C.; Steinrück, H.-P., In situ high-resolution X-ray photoelectron spectroscopy – Fundamental insights in surface reactions. *Surface Science Reports* **2013**, *68*, 446-487.
5. Roy, K.; Artiglia, L.; van Bokhoven, J. A., Ambient Pressure Photoelectron Spectroscopy: Opportunities in Catalysis from Solids to Liquids and Introducing Time Resolution. *ChemCatChem* **2018**, *10*, 666-682.
6. Yeung, K. L.; Yao, N., Scanning Probe Microscopy in Catalysis. *Journal of Nanoscience and Nanotechnology* **2004**, *4*, 647-690.
7. Zhang, Z.; Xu, P.; Yang, X.; Liang, W.; Sun, M., Surface plasmon-driven photocatalysis in ambient, aqueous and high-vacuum monitored by SERS and TERS. *Journal of Photochemistry and Photobiology C: Photochemistry Reviews* **2016**, *27*, 100-112.
8. Frenkel, A. I.; Rodriguez, J. A.; Chen, J. G., Synchrotron Techniques for In Situ Catalytic Studies: Capabilities, Challenges, and Opportunities. *ACS Catalysis* **2012**, *2*, 2269-2280.
9. González-Rubio, G.; Guerrero-Martínez, A.; Liz-Marzán, L. M., Reshaping, Fragmentation, and Assembly of Gold Nanoparticles Assisted by Pulse Lasers. *Accounts of Chemical Research* **2016**, *49*, 678-686.
10. Zijlstra, P.; Chon, J. W. M.; Gu, M., White light scattering spectroscopy and electron microscopy of laser induced melting in single gold nanorods. *Physical Chemistry Chemical Physics* **2009**, *11*, 5915-5921.
11. Vendelbo, S. B.; Elkjær, C. F.; Falsig, H.; Puspitasari, I.; Dona, P.; Mele, L.; Morana, B.; Nelissen, B. J.; van Rijn, R.; Creemer, J. F.; Kooyman, P. J.; Helveg, S., Visualization of oscillatory behaviour of Pt nanoparticles catalysing CO oxidation. *Nat Mater* **2014**, *13*, 884-890.
12. Asoro, M. A.; Kovar, D.; Ferreira, P. J., Effect of surface carbon coating on sintering of silver nanoparticles: in situ TEM observations. *Chemical Communications* **2014**, *50*, 4835-4838.
13. Li, Y.; Zang, L.; Jacobs, D. L.; Zhao, J.; Yue, X.; Wang, C., In situ study on atomic mechanism of melting and freezing of single bismuth nanoparticles. *Nat Commun* **2017**, *8*, 14462.
14. Schwind, M.; Langhammer, C.; Kasemo, B.; Zorić, I., Nanoplasmonic sensing and QCM-D as ultrasensitive complementary techniques for kinetic corrosion studies of aluminum nanoparticles. *Applied Surface Science* **2011**, *257*, 5679-5687.
15. Railsback, J. G.; Johnston-Peck, A. C.; Wang, J.; Tracy, J. B., Size-Dependent Nanoscale Kirkendall Effect During the Oxidation of Nickel Nanoparticles. *Acs Nano* **2010**, *4*, 1913-1920.
16. Wang, W.; Dahl, M.; Yin, Y., Hollow Nanocrystals through the Nanoscale Kirkendall Effect. *Chem Mater* **2013**, *25*, 1179-1189.
17. Niu, W.; Li, Z.-Y.; Shi, L.; Liu, X.; Li, H.; Han, S.; Chen, J.; Xu, G., Seed-Mediated Growth of Nearly Monodisperse Palladium Nanocubes with Controllable Sizes. *Crystal Growth & Design* **2008**, *8*, 4440-4444.

18. Roldan Cuenya, B.; Behafarid, F., Nanocatalysis: size- and shape-dependent chemisorption and catalytic reactivity. *Surface Science Reports* **2015**, *70*, 135-187.
19. Masliuk, L.; Heggen, M.; Noack, J.; Girgsdies, F.; Trunschke, A.; Hermann, K. E.; Willinger, M. G.; Schlögl, R.; Lunkenbein, T., Structural Complexity in Heterogeneous Catalysis: Cataloging Local Nanostructures. *The Journal of Physical Chemistry C* **2017**, *121*, 24093-24103.
20. Zhou, X.; Andoy, N. M.; Liu, G.; Choudhary, E.; Han, K.-S.; Shen, H.; Chen, P., Quantitative super-resolution imaging uncovers reactivity patterns on single nanocatalysts. *Nature Nanotechnology* **2012**, *7*, 237-241.
21. Sambur, J. B.; Chen, P., Approaches to Single-Nanoparticle Catalysis. *Annu Rev Phys Chem* **2014**, *65*, 395-422.
22. Hartman, T.; Wondergem, C. S.; Kumar, N.; van den Berg, A.; Weckhuysen, B. M., Surface- and Tip-Enhanced Raman Spectroscopy in Catalysis. *The Journal of Physical Chemistry Letters* **2016**, *7*, 1570-1584.
23. Roeffaers, M. B. J.; Sels, B. F.; Uji-i, H.; De Schryver, F. C.; Jacobs, P. A.; De Vos, D. E.; Hofkens, J., Spatially resolved observation of crystal-face-dependent catalysis by single turnover counting. *Nature* **2006**, *439*, 572-575.
24. Hendriks, F. C.; Mohammadian, S.; Ristanović, Z.; Kalirai, S.; Meirer, F.; Vogt, E. T. C.; Bruijninx, P. C. A.; Gerritsen, H. C.; Weckhuysen, B. M., Integrated Transmission Electron and Single-Molecule Fluorescence Microscopy Correlates Reactivity with Ultrastructure in a Single Catalyst Particle. *Angewandte Chemie International Edition* **2018**, *57*, 257-261.
25. van Schroyen Lantman, E. M.; Deckert-Gaudig, T.; Mank, A. J. G.; Deckert, V.; Weckhuysen, B. M., Catalytic processes monitored at the nanoscale with tip-enhanced Raman spectroscopy. *Nature Nanotechnology* **2012**, *7*, 583-586.
26. Karim, W.; Spreafico, C.; Kleibert, A.; Gobrecht, J.; VandeVondele, J.; Ekinci, Y.; van Bokhoven, J. A., Catalyst support effects on hydrogen spillover. *Nature* **2017**, *541*, 68-71.
27. Ringe, E.; Sharma, B.; Henry, A.-I.; Marks, L. D.; Van Duyne, R. P., Single nanoparticle plasmonics. *Physical Chemistry Chemical Physics* **2013**, *15*, 4110-4129.
28. Johánek, V.; Laurin, M.; Grant, A. W.; Kasemo, B.; Henry, C. R.; Libuda, J., Fluctuations and Bistabilities on Catalyst Nanoparticles. *Science* **2004**, *304*, 1639-1644.
29. Alayoglu, S.; Krier, J. M.; Michalak, W. D.; Zhu, Z.; Gross, E.; Somorjai, G. A., In Situ Surface and Reaction Probe Studies with Model Nanoparticle Catalysts. *ACS Catalysis* **2012**, *2*, 2250-2258.
30. Liz-Marzán, L. M., Tailoring Surface Plasmons through the Morphology and Assembly of Metal Nanoparticles. *Langmuir* **2006**, *22*, 32-41.
31. Hanske, C.; Sanz-Ortiz, M. N.; Liz-Marzán, L. M., Silica-Coated Plasmonic Metal Nanoparticles in Action. *Adv Mater* **2018**, *30*, 1707003.
32. Zopf, D.; Jatschka, J.; Dathe, A.; Jahr, N.; Fritzsche, W.; Stranik, O., Hyperspectral imaging of plasmon resonances in metallic nanoparticles. *Biosensors and Bioelectronics* **2016**, *81*, 287-293.
33. Fritzsche, J.; Albinsson, D.; Fritzsche, M.; Antosiewicz, T. J.; Westerlund, F.; Langhammer, C., Single Particle Nanoplasmonic Sensing in Individual Nanofluidic Channels. *Nano Letters* **2016**, *16*, 7857-7864.

34. Pini, V.; Kosaka, P. M.; Ruz, J. J.; Malvar, O.; Encinar, M.; Tamayo, J.; Calleja, M., Spatially multiplexed dark-field microspectrophotometry for nanoplasmonics. *Scientific Reports* **2016**, *6*, 22836.
35. Kirchner, S. R.; Smith, K. W.; Hoener, B. S.; Collins, S. S. E.; Wang, W.; Cai, Y.-Y.; Kinnear, C.; Zhang, H.; Chang, W.-S.; Mulvaney, P.; Landes, C. F.; Link, S., Snapshot Hyperspectral Imaging (SHI) for Revealing Irreversible and Heterogeneous Plasmonic Processes. *The Journal of Physical Chemistry C* **2018**, *122*, 6865-6875.
36. Taylor, A. B.; Zijlstra, P., Single-Molecule Plasmon Sensing: Current Status and Future Prospects. *ACS Sensors* **2017**, *2*, 1103-1122.
37. Mayer, K. M.; Hafner, J. H., Localized Surface Plasmon Resonance Sensors. *Chemical Reviews* **2011**, *111*, 3828-3857.
38. Tittl, A.; Giessen, H.; Liu, N., Plasmonic gas and chemical sensing. In *Nanophotonics*, 2014; Vol. 3, pp 157-180.
39. Larsson, E.; Syrenova, S.; Langhammer, C., Nanoplasmonic sensing for nanomaterials science. *Nanophotonics* **2012**, *1*, 249.
40. Tian, L. M.; Fei, M.; Kattumenu, R.; Abbas, A.; Singamaneni, S., Gold nanorods as nanotransducers to monitor the growth and swelling of ultrathin polymer films. *Nanotechnology* **2012**, *23*, 255502.
41. Langhammer, C.; Zorić, I.; Kasemo, B.; Clemens, B. M., Hydrogen Storage in Pd Nanodisks Characterized with a Novel Nanoplasmonic Sensing Scheme. *Nano Letters* **2007**, *7*, 3122-3127.
42. Zorić, I.; Larsson, E. M.; Kasemo, B.; Langhammer, C., Localized Surface Plasmons Shed Light on Nanoscale Metal Hydrides. *Adv Mater* **2010**, *22*, 4628-4633.
43. Larsson, E. M.; Edvardsson, M. E. M.; Langhammer, C.; Zoric, I.; Kasemo, B., A combined nanoplasmonic and electrodeless quartz crystal microbalance setup. *Review of Scientific Instruments* **2009**, *80*, 125105.
44. Dalacu, D.; Martinu, L., Temperature dependence of the surface plasmon resonance of Au/SiO<sub>2</sub> nanocomposite films. *Applied Physics Letters* **2000**, *77*, 4283-4285.
45. Suh, J. Y.; Donev, E. U.; Ferrara, D. W.; Tetz, K. A.; Feldman, L. C.; Haglund, R. F., Modulation of the gold particle-plasmon resonance by the metal-semiconductor transition of vanadium dioxide. *J. Opt. A-Pure Appl. Opt.* **2008**, *10*, 055202.
46. Szwarcman, D.; Vestler, D.; Markovich, G., The Size-Dependent Ferroelectric Phase Transition in BaTiO<sub>3</sub> Nanocrystals Probed by Surface Plasmons. *Acs Nano* **2011**, *5*, 507-515.
47. Langhammer, C.; Larsson, E. M.; Kasemo, B.; Zorić, I., Indirect Nanoplasmonic Sensing: Ultrasensitive Experimental Platform for Nanomaterials Science and Optical Nanocalorimetry. *Nano Letters* **2010**, *10*, 3529-3538.
48. Nugroho, F. A. A.; Diaz de Zerio Mendaza, A.; Lindqvist, C.; Antosiewicz, T. J.; Müller, C.; Langhammer, C., Plasmonic Nanospectroscopy for Thermal Analysis of Organic Semiconductor Thin Films. *Anal Chem* **2017**, *89*, 2575-2582.
49. Chan, G. H.; Zhao, J.; Hicks, E. M.; Schatz, G. C.; Van Duyne, R. P., Plasmonic Properties of Copper Nanoparticles Fabricated by Nanosphere Lithography. *Nano Letters* **2007**, *7*, 1947-1952.
50. Tabib Zadeh Adibi, P.; Pingel, T.; Olsson, E.; Grönbeck, H.; Langhammer, C., Plasmonic Nanospectroscopy of Platinum Catalyst Nanoparticle Sintering in a Mesoporous Alumina Support. *Acs Nano* **2016**, *10*, 5063-5069.

51. Larsson, E. M.; Millet, J.; Gustafsson, S.; Skoglundh, M.; Zhdanov, V. P.; Langhammer, C., Real Time Indirect Nanoplasmonic in Situ Spectroscopy of Catalyst Nanoparticle Sintering. *Acs Catalysis* **2012**, *2*, 238-245.
52. Zheng, Y. B.; Huang, T. J.; Desai, A. Y.; Wang, S. J.; Tan, L. K.; Gao, H.; Huan, A. C. H., Thermal behavior of localized surface plasmon resonance of Au/TiO<sub>2</sub> core/shell nanoparticle arrays. *Applied Physics Letters* **2007**, *90*, 183117.
53. Gusak, V.; Heiniger, L. P.; Graetzel, M.; Langhammer, C.; Kasemo, B., Time-Resolved Indirect Nanoplasmonic Sensing Spectroscopy of Dye Molecule Interactions with Dense and Mesoporous TiO<sub>2</sub> Films. *Nano Letters* **2012**, *12*, 2397-2403.
54. Herrmann Lars, O.; Baumberg Jeremy, J., Watching Single Nanoparticles Grow in Real Time through Supercontinuum Spectroscopy. *Small* **2013**, *9*, 3743-3747.
55. Liu, Y.; Huang, C. Z., Real-Time Dark-Field Scattering Microscopic Monitoring of the in Situ Growth of Single Ag@Hg Nanoalloys. *Acs Nano* **2013**, *7*, 11026-11034.
56. McFarland, A. D.; Van Duyne, R. P., Single Silver Nanoparticles as Real-Time Optical Sensors with Zeptomole Sensitivity. *Nano Letters* **2003**, *3*, 1057-1062.
57. Garcia, M. A., Surface plasmons in metallic nanoparticles: fundamentals and applications. *Journal of Physics D: Applied Physics* **2011**, *44*, 283001.
58. Bohren, C. F.; Huffman, D. R., *Absorption and Scattering of Light by Small Particles*. Wiley-VCH Verlag GmbH: Weinheim, Germany, 1998.
59. Willets, K. A.; Van Duyne, R. P., Localized Surface Plasmon Resonance Spectroscopy and Sensing. *Annu Rev Phys Chem* **2007**, *58*, 267-297.
60. Langhammer, C.; Larsson, E. M., Nanoplasmonic In Situ Spectroscopy for Catalysis Applications. *ACS Catalysis* **2012**, *2*, 2036-2045.
61. Wadell, C.; Syrenova, S.; Langhammer, C., Plasmonic Hydrogen Sensing with Nanostructured Metal Hydrides. *Acs Nano* **2014**, *8*, 11925-11940.
62. Palm, K. J.; Murray, J. B.; Narayan, T. C.; Munday, J. N., Dynamic Optical Properties of Metal Hydrides. *Acs Photonics* **2018**, *5*, 4677-4686.
63. Rodal-Cedeira, S.; Montes-García, V.; Polavarapu, L.; Solís, D. M.; Heidari, H.; La Porta, A.; Angiola, M.; Martucci, A.; Taboada, J. M.; Obelleiro, F.; Bals, S.; Pérez-Juste, J.; Pastoriza-Santos, I., Plasmonic Au@Pd Nanorods with Boosted Refractive Index Susceptibility and SERS Efficiency: A Multifunctional Platform for Hydrogen Sensing and Monitoring of Catalytic Reactions. *Chem Mater* **2016**, *28*, 9169-9180.
64. Nugroho, F. A. A.; Darmadi, I.; Cusinato, L.; Susarrey-Arce, A.; Schreuders, H.; Bannenberg, L. J.; da Silva Fanta, A. B.; Kadkhodazadeh, S.; Wagner, J. B.; Antosiewicz, T. J.; Hellman, A.; Zhdanov, V. P.; Dam, B.; C., L., Metal - Polymer Hybrid Nanomaterials for Plasmonic Ultrafast Hydrogen Detection. *Nat Mater* **2019**, *18*, 489-495.
65. Poyli, M. A.; Silkin, V. M.; Chernov, I. P.; Echenique, P. M.; Muiño, R. D.; Aizpurua, J., Multiscale Theoretical Modeling of Plasmonic Sensing of Hydrogen Uptake in Palladium Nanodisks. *The Journal of Physical Chemistry Letters* **2012**, *3*, 2556-2561.
66. Liu, N.; Tang, M. L.; Hentschel, M.; Giessen, H.; Alivisatos, A. P., Nanoantenna-enhanced gas sensing in a single tailored nanofocus. *Nat Mater* **2011**, *10*, 631-636.
67. Tittl, A.; Yin, X.; Giessen, H.; Tian, X.-D.; Tian, Z.-Q.; Kremers, C.; Chigrin, D. N.; Liu, N., Plasmonic Smart Dust for Probing Local Chemical Reactions. *Nano Letters* **2013**, *13*, 1816-1821.

68. Shegai, T.; Langhammer, C., Hydride Formation in Single Palladium and Magnesium Nanoparticles Studied By Nanoplasmonic Dark-Field Scattering Spectroscopy. *Adv Mater* **2011**, *23*, 4409-4414.
69. Langhammer, C.; Kasemo, B.; Zorić, I., Absorption and scattering of light by Pt, Pd, Ag, and Au nanodisks: Absolute cross sections and branching ratios. *The Journal of Chemical Physics* **2007**, *126*, 194702.
70. Tittl, A.; Kremers, C.; Dorfmüller, J.; Chigrin, D. N.; Giessen, H., Spectral shifts in optical nanoantenna-enhanced hydrogen sensors. *Opt. Mater. Express* **2012**, *2*, 111-118.
71. Tang, M. L.; Liu, N.; Dionne, J. A.; Alivisatos, A. P., Observations of Shape-Dependent Hydrogen Uptake Trajectories from Single Nanocrystals. *Journal of the American Chemical Society* **2011**, *133*, 13220-13223.
72. Li, J.-F.; Zhang, Y.-J.; Ding, S.-Y.; Panneerselvam, R.; Tian, Z.-Q., Core-Shell Nanoparticle-Enhanced Raman Spectroscopy. *Chemical Reviews* **2017**, *117*, 5002-5069.
73. Baldi, A.; Narayan, T. C.; Koh, A. L.; Dionne, J. A., In situ detection of hydrogen-induced phase transitions in individual palladium nanocrystals. *Nat Mater* **2014**, *13*, 1143-1148.
74. Narayan, T. C.; Baldi, A.; Koh, A. L.; Sinclair, R.; Dionne, J. A., Reconstructing solute-induced phase transformations within individual nanocrystals. *Nat Mater* **2016**, *15*, 768-774.
75. Syrenova, S.; Wadell, C.; Nugroho, F. A. A.; Gschneidner, T. A.; Diaz Fernandez, Y. A.; Nalin, G.; Switlik, D.; Westerlund, F.; Antosiewicz, T. J.; Zhdanov, V. P.; Moth-Poulsen, K.; Langhammer, C., Hydride formation thermodynamics and hysteresis in individual Pd nanocrystals with different size and shape. *Nat Mater* **2015**, *14*, 1236-1244.
76. Alekseeva, S.; Fanta, A. B. d. S.; Iandolo, B.; Antosiewicz, T. J.; Nugroho, F. A. A.; Wagner, J. B.; Burrows, A.; Zhdanov, V. P.; Langhammer, C., Grain boundary mediated hydriding phase transformations in individual polycrystalline metal nanoparticles. *Nat Commun* **2017**, *8*, 1084.
77. Gschneidner, T. A.; Fernandez, Y. A. D.; Syrenova, S.; Westerlund, F.; Langhammer, C.; Moth-Poulsen, K., A Versatile Self-Assembly Strategy for the Synthesis of Shape-Selected Colloidal Noble Metal Nanoparticle Heterodimers. *Langmuir* **2014**, *30*, 3041-3050.
78. Hayee, F.; Narayan, T. C.; Nadkarni, N.; Baldi, A.; Koh, A. L.; Bazant, M. Z.; Sinclair, R.; Dionne, J. A., In-situ visualization of solute-driven phase coexistence within individual nanorods. *Nat Commun* **2018**, *9*, 1775.
79. Narayan, T. C.; Hayee, F.; Baldi, A.; Leen Koh, A.; Sinclair, R.; Dionne, J. A., Direct visualization of hydrogen absorption dynamics in individual palladium nanoparticles. *Nat Commun* **2017**, *8*, 14020.
80. Sytwu, K.; Hayee, F.; Narayan, T. C.; Koh, A. L.; Sinclair, R.; Dionne, J. A., Visualizing Facet-Dependent Hydrogenation Dynamics in Individual Palladium Nanoparticles. *Nano Letters* **2018**, *18*, 5357-5363.
81. Vadai, M.; Angell, D. K.; Hayee, F.; Sytwu, K.; Dionne, J. A., In-situ observation of plasmon-controlled photocatalytic dehydrogenation of individual palladium nanoparticles. *Nat Commun* **2018**, *9*, 4658.
82. Sherry, L. J.; Chang, S.-H.; Schatz, G. C.; Van Duyne, R. P.; Wiley, B. J.; Xia, Y., Localized Surface Plasmon Resonance Spectroscopy of Single Silver Nanocubes. *Nano Letters* **2005**, *5*, 2034-2038.



83. Sherry, L. J.; Jin, R.; Mirkin, C. A.; Schatz, G. C.; Van Duyne, R. P., Localized Surface Plasmon Resonance Spectroscopy of Single Silver Triangular Nanoprisms. *Nano Letters* **2006**, *6*, 2060-2065.
84. Duyne, R. P. V.; Haes, A. J.; McFarland, A. D. In *Nanoparticle optics: sensing with nanoparticle arrays and single nanoparticles*, Optical Science and Technology, SPIE's 48th Annual Meeting, SPIE: 2003; p 11.
85. Sönnichsen, C.; Geier, S.; Hecker, N. E.; Plessen, G. v.; Feldmann, J.; Ditlbacher, H.; Lamprecht, B.; Krenn, J. R.; Aussenegg, F. R.; Chan, V. Z.-H.; Spatz, J. P.; Möller, M., Spectroscopy of single metallic nanoparticles using total internal reflection microscopy. *Applied Physics Letters* **2000**, *77*, 2949-2951.
86. Jing, C.; Gu, Z.; Ying, Y.-L.; Li, D.-W.; Zhang, L.; Long, Y.-T., Chrominance to Dimension: A Real-Time Method for Measuring the Size of Single Gold Nanoparticles. *Anal Chem* **2012**, *84*, 4284-4291.
87. Gu, Z.; Jing, C.; Ying, Y.-L.; He, P.; Long, Y.-T., In situ High Throughput Scattering Light Analysis of Single Plasmonic Nanoparticles in Living Cells. *Theranostics* **2015**, *5*, 188-195.
88. Bingham, J. M.; Willets, K. A.; Shah, N. C.; Andrews, D. Q.; Van Duyne, R. P., Localized Surface Plasmon Resonance Imaging: Simultaneous Single Nanoparticle Spectroscopy and Diffusional Dynamics. *The Journal of Physical Chemistry C* **2009**, *113*, 16839-16842.
89. Liu, G. L.; Doll, J. C.; Lee, L. P., High-speed multispectral imaging of nanoplasmonic array. *Opt. Express* **2005**, *13*, 8520-8525.
90. Beuwer, M. A.; Prins, M. W. J.; Zijlstra, P., Stochastic Protein Interactions Monitored by Hundreds of Single-Molecule Plasmonic Biosensors. *Nano Letters* **2015**, *15*, 3507-3511.
91. Collins, S. S. E.; Wei, X.; McKenzie, T. G.; Funston, A. M.; Mulvaney, P., Single Gold Nanorod Charge Modulation in an Ion Gel Device. *Nano Letters* **2016**, *16*, 6863-6869.
92. Dynamics. In *Handbook of Surface Science*, Hasselbrink, E.; Lundqvist, B. I., Eds. Elsevier: 2008; Vol. 3, pp 1-1015.
93. Novo, C.; Funston, A. M.; Mulvaney, P., Direct observation of chemical reactions on single gold nanocrystals using surface plasmon spectroscopy. *Nat Nano* **2008**, *3*, 598-602.
94. Li, K.; Wang, K.; Qin, W.; Deng, S.; Li, D.; Shi, J.; Huang, Q.; Fan, C., DNA-Directed Assembly of Gold Nanohalo for Quantitative Plasmonic Imaging of Single-Particle Catalysis. *Journal of the American Chemical Society* **2015**, *137*, 4292-4295.
95. Seo, D.; Park, G.; Song, H., Plasmonic Monitoring of Catalytic Hydrogen Generation by a Single Nanoparticle Probe. *Journal of the American Chemical Society* **2012**, *134*, 1221-1227.
96. Xiong, B.; Zhou, R.; Hao, J.; Jia, Y.; He, Y.; Yeung, E. S., Highly sensitive sulphide mapping in live cells by kinetic spectral analysis of single Au-Ag core-shell nanoparticles. *Nat Commun* **2013**, *4*, 1708.
97. Eo, M.; Baek, J.; Song, H. D.; Lee, S.; Yi, J., Quantification of electron transfer rates of different facets on single gold nanoparticles during catalytic reactions. *Chemical Communications* **2013**, *49*, 5204-5206.
98. Cheng, J.; Liu, Y.; Cheng, X. D.; He, Y.; Yeung, E. S., Real Time Observation of Chemical Reactions of Individual Metal Nanoparticles with High-Throughput Single Molecule Spectral Microscopy. *Anal Chem* **2010**, *82*, 8744-8749.

99. Jing, C.; Rawson, F. J.; Zhou, H.; Shi, X.; Li, W.-H.; Li, D.-W.; Long, Y.-T., New Insights into Electrocatalysis Based on Plasmon Resonance for the Real-Time Monitoring of Catalytic Events on Single Gold Nanorods. *Anal Chem* **2014**, *86*, 5513-5518.
100. Jing, C.; Gu, Z.; Long, Y.-T., Imaging electrocatalytic processes on single gold nanorods. *Faraday Discussions* **2016**, *193*, 371-385.
101. Wang, J.-G.; Fossey, J. S.; Li, M.; Li, D.-W.; Ma, W.; Ying, Y.-L.; Qian, R.-C.; Cao, C.; Long, Y.-T., Real-time plasmonic monitoring of electrocatalysis on single nanorods. *Journal of Electroanalytical Chemistry* **2016**, *781*, 257-264.
102. Wonner, K.; Evers, M. V.; Tschulik, K., Simultaneous Opto- and Spectro-Electrochemistry: Reactions of Individual Nanoparticles Uncovered by Dark-Field Microscopy. *Journal of the American Chemical Society* **2018**, *140*, 12658-12661.
103. Larsson, E. M.; Langhammer, C.; Zorić, I.; Kasemo, B., Nanoplasmonic Probes of Catalytic Reactions. *Science* **2009**, *326*, 1091-1094.
104. Fredriksson, H. O. A.; Larsson Langhammer, E. M.; Niemantsverdriet, J. W., Reduction of Cu-Promoted Fe Model Catalysts Studied by In Situ Indirect Nanoplasmonic Sensing and X-ray Photoelectron Spectroscopy. *The Journal of Physical Chemistry C* **2015**, *119*, 4085-4094.
105. Bu, Y.; Niemantsverdriet, J. W. H.; Fredriksson, H. O. A., Cu Model Catalyst Dynamics and CO Oxidation Kinetics Studied by Simultaneous in Situ UV-Vis and Mass Spectroscopy. *ACS Catalysis* **2016**, *6*, 2867-2876.
106. Collins, S. S. E.; Cittadini, M.; Pecharrómán, C.; Martucci, A.; Mulvaney, P., Hydrogen Spillover between Single Gold Nanorods and Metal Oxide Supports: A Surface Plasmon Spectroscopy Study. *Acs Nano* **2015**, *9*, 7846-7856.
107. Lerch, S.; Reinhard, B. M., Effect of interstitial palladium on plasmon-driven charge transfer in nanoparticle dimers. *Nat Commun* **2018**, *9*, 1608.
108. Zorić, I.; Zäch, M.; Kasemo, B.; Langhammer, C., Gold, Platinum, and Aluminum Nanodisk Plasmons: Material Independence, Subradiance, and Damping Mechanisms. *Acs Nano* **2011**, *5*, 2535-2546.
109. Wadell, C.; Antosiewicz, T. J.; Langhammer, C., Optical Absorption Engineering in Stacked Plasmonic Au-SiO<sub>2</sub>-Pd Nanoantennas. *Nano Letters* **2012**, *12*, 4784-4790.
110. Boyer, D.; Tamarat, P.; Maali, A.; Lounis, B.; Orrit, M., Photothermal Imaging of Nanometer-Sized Metal Particles Among Scatterers. *Science* **2002**, *297*, 1160-1163.
111. Young, G.; Hundt, N.; Cole, D.; Fineberg, A.; Andrecka, J.; Tyler, A.; Olerinyova, A.; Ansari, A.; Marklund, E. G.; Collier, M. P.; Chandler, S. A.; Tkachenko, O.; Allen, J.; Crispin, M.; Billington, N.; Takagi, Y.; Sellers, J. R.; Eichmann, C.; Selenko, P.; Frey, L.; Riek, R.; Galpin, M. R.; Struwe, W. B.; Benesch, J. L. P.; Kukura, P., Quantitative mass imaging of single biological macromolecules. *Science* **2018**, *360*, 423-427.
112. Ament, I.; Prasad, J.; Henkel, A.; Schmachtel, S.; Sönnichsen, C., Single Unlabeled Protein Detection on Individual Plasmonic Nanoparticles. *Nano Letters* **2012**, *12*, 1092-1095.
113. Aćimović, S. S.; Šípová-Jungová, H.; Emilsson, G.; Shao, L.; Dahlin, A. B.; Käll, M.; Antosiewicz, T. J., Antibody-Antigen Interaction Dynamics Revealed by Analysis of Single-Molecule Equilibrium Fluctuations on Individual Plasmonic Nanoparticle Biosensors. *Acs Nano* **2018**, *12*, 9958-9965.

114. Ortega-Arroyo, J.; Kukura, P., Interferometric scattering microscopy (iSCAT): new frontiers in ultrafast and ultrasensitive optical microscopy. *Physical Chemistry Chemical Physics* **2012**, *14*, 15625-15636.
115. Shashkova, S.; Leake, M. C., Single-molecule fluorescence microscopy review: shedding new light on old problems. *Bioscience Reports* **2017**, *37*, BSR20170031.

## TOC GRAPHICS

